S-JSCC: A Digital Joint Source-Channel Coding Framework based on Spiking Neural Network

Mengyang Wang, Jiahui Li, *Member, IEEE*, Mengyao Ma, *Member, IEEE*,
and Xiaopeng Fan, *Senior Member, IEEE*

Abstract—Nowadays, deep learning-based joint source-channel coding (JSCC) is getting attention, and it shows excellent performance compared with separate source and channel coding (SSCC). However, most JSCC works are only designed, trained, and tested on additive white Gaussian noise (AWGN) channels to transmit analog signals. In current communication systems, digital signals are considered more. Hence, it is necessary to design an end-to-end JSCC framework for digital signal transmission. In this paper, we propose a digital JSCC framework (S-JSCC) based on spiking neural network (SNN) to tackle this problem. The SNN is used to compress the feature of the deep model, and the compressed results are transmitted over digital channels such as binary symmetric channel (BSC) and binary erasure channel (BEC). Since the outputs of SNN are binary spikes, the framework can be applied directly to digital channels without extra quantization. Moreover, we propose a new spiking neuron and regularization method to improve the performance and robustness of the system. The experimental results show that under digital channels, the proposed S-JSCC framework performs better than the state-of-the-art convolution neural network (CNN)-based JSCC framework, which needs extra quantization.

Index Terms—Digital communication, deep joint source-channel coding, spiking neural network

I. INTRODUCTION

WITH the rapid development of deep learning (DL) [1], artificial neural networks (ANNs) such as convolutional neural networks (CNNs), fully connected neural networks (FCNNs), and recurrent neural networks (RNNs) have become more and more important. Compared with traditional algorithms, ANN-based models can solve problems in computer vision (CV), natural language processing (NLP), and other fields more accurately and effectively. Moreover, ANNs also play a role in collaborative intelligence (CI) [2] and physical layer communication [3].

In CI, the problem is that the deep model is too complex and computationally expensive. Therefore, the model is divided into two parts: the mobile device and the edge server. The two parts complete the computation of the whole model collaboratively. The mobile device obtains input information such as images and videos, and extracts intermediate feature by using the mobile device part of the deep model. The intermediate feature is then sent to the edge server for subsequent task inference. However, transmitting the original intermediate feature may consume a large amount of channel bandwidth,

Mengyang Wang and Xiaopeng Fan is with the School of Computer Science, Harbin Institute of Technology, Harbin 150001, China (e-mail: mywang1996@outlook.com; fxp@hit.edu.cn). Jiahui Li and Mengyao Ma are with the Wireless Technology Lab, Huawei, Shenzhen 518129, China (e-mail: lijiahui666@huawei.com; ma.mengyao@huawei.com).

so we need to compress it before transmission. In [4] and [5], the feature is treated as a video with multiple frames, and then HEVC-Intra and HEVC-Inter [6] of the video coding framework are used to compress it, respectively. In [7] and [8], the feature is rearranged to form a tiled image, then image codecs such as PNG [9] and JPEG [10] are used to compress it. Apart from these traditional methods, the CNN-based model called auto-encoder (AE) can also reduce and restore the dimension of the feature [11]. The butterfly unit proposed in [12] uses two convolution layers to reduce the feature size at mobile service, and restore it at edge server. To further improve model compression capability, the bottlenet unit [13] uses JPEG to compress the compression result of the AE. Moreover, to compress multi-scale features, the framework in [14] first merges them into one large feature and then compresses the large feature with AE. Although these works reduce the feature size, none of them takes channel noise interference into account during transmission. Therefore, in order to achieve high compression rate and anti-noise capability simultaneously, the joint source-channel coding (JSCC) technique is proposed.

In traditional communication systems, source coding and channel coding are two independent steps. The purpose of source coding is to remove the redundant information in the source as much as possible, while channel coding reintroduces redundancy to protect the information from channel noise. According to Shannon's separation theorem, the two-step separate approach is optimal theoretically in the asymptotic limit of infinitely long source and channel blocks [15]. However, the blocklength is finite in practice, and JSCC's performance in this scenario has been shown to outperform the separate approach [16]. For a deeper study of JSCC, some CNN-based JSCC models are proposed. In [17], an end-to-end JSCC framework for transmitting images is built by multi-layer AE, and an additive white Gaussian noise (AWGN) layer is placed between the encoder and decoder to simulate channel interference. By training the model with noise, the input image is compressed and transmitted robustly through the AWGN channel. Moreover, the JSCC model overcomes the 'cliff effect' of the separate method. As the research continues, [18] and [19] propose JSCC models to adapt channels with different signal-to-noise ratios (SNRs). [18] proposes a new training strategy, which uses a channel with randomly varying SNRs to train the model. [19] proposes a new attention module that uses SNR to enhance the robustness of feature encoding. Both works show robustness to different channel SNRs. Considering the distributed scenario, [20] designs a JSCC framework with two encoders, which compresses and transmits a pair of cor-

related images over independent channels and jointly recovers them by one decoder. In addition to transmitting images, the JSCC framework can also be applied to CI to compress and transmit intermediate features. [21] and [22] design AE-based JSCC models to compress the intermediate features of the image retrieval model and the classification model, respectively. Moreover, [23] and [24] design JSCC models for the intermediate features of the multi-task model and the multi-modal model. According to our investigation, most DL-based JSCC frameworks are trained and tested only on AWGN channels to transmit analog information. Although the binary erasure channel (BEC) is considered by BottleNet++ [22], it adds an additional quantization step to binarize the information prior to transmission, the additional quantization step is non-differentiable and increases computational overhead. Therefore, it is necessary to design an end-to-end JSCC framework for digital communication systems without additional quantization.

Nowadays, the spiking neural network (SNN) is seen as the third generation of neural network models [25], and it is closer to the biological neurons in the brain [26]. The communication information between spike neurons is binary spikes denoted by 0s and 1s, making the energy consumption of SNN lower than ANN. Besides, unlike ANN which only needs one time forward pass to handle the spatial information, SNN usually runs multiple time steps to utilize spatial-temporal information [27]. The spiking neuron accumulates the input as the membrane potential at each time step. When the membrane potential exceeds a threshold, the neuron will fire a spike to the neuron in the next layer and reset the membrane potential [28], [29]. Currently, SNNs are widely used for computer vision tasks, and by running multiple time steps, the performance of SNNs is very close to that of ANN models [30]–[33]. Since the output of the spiking neuron is a binary spike, it can be considered a binary encoding process of the input and does not need an additional quantization step. Based on this property, we use SNN to build an end-to-end JSCC model for binary digital channels. Although there is also research on applying SNN on JSCC, it mainly focuses on analog communication and does not make full use of the property of SNN [34].

In this paper, we propose a new JSCC model based on SNN: S-JSCC, which compresses and transmits features of deep models over digital channels under CI scenario. To improve the task performance and robustness of the model, we regularize the firing rate of the compressed result and propose a new spiking neuron to help convert the spiking features into float features. This is the first work to build an end-to-end digital JSCC model. The main contributions of this paper are summarized as follows:

1) A digital JSCC framework S-JSCC is constructed based on SNN. With this framework, we can transmit deep features over digital channels without an additional quantization step.
2) We design a new Integrate and Hybrid Fire (IHF) neuron and regularize the firing rate of the JSCC encoder output to improve the task performance and robustness of the model.
3) Compared with the ANN-based JSCC model with an

additional quantization step, S-JSCC model achieves higher task performance under poor channel conditions and gets very close task performance under good channel conditions.
4) The S-JSCC model can be combined with most deep models, to compress and transmit features over digital channels. This work also points out a new direction for the follow-up study of JSCC.

II. BACKGROUND

A. Digital Channels

Channels that transmit digital signals are called digital channels. The signal changes in digital channels are discrete, and for binary channels, there are only two states in the whole signal: high level and low level. The high level is represented by a logic 1 and the low level is represented by a logic 0. In the digital communication system, there are two typical channel models: Binary Symmetric Channel (BSC) and Binary Erasure Channel (BEC).

In the digital channel, an error occurs when the input bit of the channel is inconsistent with the output bit of the channel. We first consider the BSC, and the bit error rate is used to model the probability of errors occurring when transmitting bits in the BSC. In the BSC, every bit in the bit stream may have an error independently. On the other hand, the BEC erases the bit into a corrupted symbol e (e.g., $0 \rightarrow e$) independently with a probability called bit erasure rate. In our experiments, the value of the erased bit is set to be 0 or 1 with equal probability on the decoder side. In BEC, the unerased bits are transmitted correctly [35].

B. Spiking Neuron Models

The spiking neuron is the basic computing unit of SNN. Many spiking neuron models are proposed to simulate the activity of neurons in the human brain. There are three main steps for the spiking neuron: charge, fire, and reset [27]. At each timestep, the three steps are executed in sequence. We will introduce these steps one by one.

At first, the spiking neuron accumulates the weighted input at the current timestep as membrane potential, and the iterative model of charging can be modeled as

$$m_i^t = \lambda m_i^{t-1} + I_{i-1}, \tag{1}$$

where m_i^t represents the membrane potential of ith neuron at timestep t, and I_{i-1} is the weighted input from previous layer. The Integrate-Fire (IF) [36] and Leaky Integrate-Fire (LIF) [37] model are the most common neuronal models. The λ is the decay factor, and it is set to 1 for IF and less than 1 for LIF.

Apart from charging, the fire and reset steps of IF and LIF are the same. The fire and reset steps can be modeled as

$$O_i^t = \begin{cases} 1, & m_i^t > V_{th}, \\ 0, & \text{otherwise,} \end{cases} \tag{2}$$

$$m_i^t = \begin{cases} (1 - O_i^t)m_i^t + O_i^t V_{reset} & \text{(hard reset)}, \\ m_i^t - O_i^t V_{th} & \text{(soft reset)}, \end{cases} \tag{3}$$
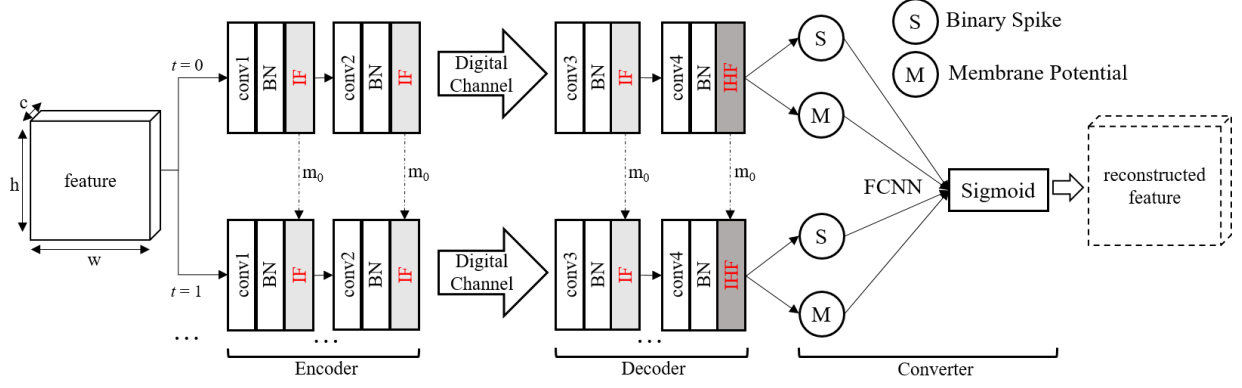
Fig. 1. The architecture of the S-JSCC model over digital channel.

where O_i^t of Eq. 2 is the output spike of neuron i, and V_{th} is the firing threshold of the neuron. When the membrane potential exceeds the threshold, the neuron will fire a spike at the current timestep. The membrane potential will be reset after firing a spike. There are two reset methods as shown in Eq. 3: hard reset and soft reset. In hard reset, the membrane potential is set directly to the preset value V_{reset} [38]. On the other hand, the membrane potential is subtracted by the threshold V_{th} in soft reset [39]. Both of these reset methods have been widely used in SNN.

In addition to the IF and LIF that output binary spikes, there are some spiking neuron models that output analog values. The Membrane Potential (MP) neuron [40] and Leaky Integrate and Analog Fire (LIAF) neuron [41] output the membrane potential of the neuron at each timestep.

C. Training Methods of SNN

Since the fire step in spiking neuron is non-differentiable, some special training methods are proposed. Nowadays, the ANN-to-SNN conversion [30], [32], [42], [43] and backprop-agation with surrogate gradient are the two main methods [26], [40], [44].

The ANN-to-SNN method first trains the neural network with the rectified linear unit (ReLU) as the activation function, and then replaces the ReLU on the trained neural network with spiking neurons. However, the task performance of SNNs resulting from the direct conversion is generally poor. Therefore, additional operations such as normalization [45], [46] or threshold adjustment [29], [31] are required. On the other hand, backpropagation with surrogate gradient is used to train SNNs end-to-end from scratch. Spiking neurons run in forward propagation, and some continuously derivable approximation functions are used to replace the gradients of spiking neurons in the backpropagation.

III. METHODOLOGY

A. Overview of the SNN-based JSCC

The proposed S-JSCC model is shown in Fig. 1. From the figure we can see there are three parts in the S-JSCC framework: encoder, decoder, and converter.

In order for the SNN to process the information in the time dimension, the encoder and decoder run T timesteps. The input of S-JSCC can be the feature of the deep model. At each timestep, the feature is compressed by the SNN-based encoder, and the output of the encoder is transmitted through a digital channel to the decoder. The SNN-based decoder outputs two results: a reconstructed feature S composed of spikes and a reconstructed feature M composed of current membrane potential.

After the encoder and decoder run T timesteps, all outputs of the decoder are fused by an FCNN-based converter to obtain the final reconstructed feature.

The spiking neurons IF and IHF accumulate current input and the membrane potential values m_{t-1} in last timestep $t-1$ as current membrane potential m_t. In addition, all the parameters in the encoder and decoder are shared at all timesteps.

B. Details of the SNN-based JSCC

In the encoder, there are two conv-BN (Batch Normalization) -IF modules. Since the input of the encoder is a feature with float-points values, the first conv-BN-IF is used to encode the values into spikes (e.g. direct encoding [45], [47]) and preliminarily compress the feature at each timestep. Then the second conv-BN-IF further compresses the spiking feature after the conversion. It is assumed that the dimension of the input feature is (c, h, w), corresponding to (channel, height, width), and the feature dimensions of the first module and the second module are (c_1, h_1, w_1) and (c_2, h_2, w_2), respectively. During encoding, the size relationship among these dimensions is as follows: $c \times h \times w > c_1 \times h_1 \times w_1 > c_2 \times h_2 \times w_2$.

The encoded result composed of binary spikes is transmitted directly to the decoder through digital channels such as BSC or BEC at each timestep. Besides, the amount of data transmitted on the channel at each timestep is $c_2 \times h_2 \times w_2$ bits.

The decoder receives and decompresses interfered information. Similar to the encoder, there are two modules in the decoder. The first conv-BN-IF preliminarily decompresses the received spiking feature, and the output feature dimension is (c_1, h_1, w_1). Then the second module conv-BN-IHF further decompresses the spiking feature and outputs two features: the

feature S composed of spikes and the feature M composed of current membrane potential. Although these two features have different values, they have the same dimension as the original feature, that is, (c, h, w). It is important to note that IHF neuron is a new spiking neuron proposed in this paper, and we will introduce it in next section.

After the encoder and decoder run T timesteps, there are $2T$ output features totally. In order to obtain the final reconstructed feature, an FCNN-based converter is used to perform a weighted summation of all output features. Then, the weighted summation is input into the Sigmoid activation function to obtain the final reconstructed feature.

C. Integrate and Hybrid Fire neuron (IHF)

In our framework, the output features of the decoder at all time steps need to be fused and converted to one reconstructed floating-point feature. Based on our observation, we find that both IF which outputs only binary spikes, and LIAF which outputs only membrane potential values lose some information. Therefore, we want to combine these two neurons for better results.

In order to make full use of the information of the spiking neurons, we propose an IHF neuron that outputs spikes and membrane potential values simultaneously. The first three working steps of the IHF neuron are identical to the IF neuron, and IHF adds another output step after resetting the membrane potential. The added step outputs the current membrane potential value. Thus, IHF can be considered as a combination of IF neuron and LIAF neuron.

The change of IHF membrane potential with soft reset over timestep is shown in Fig. 2. We can find that the IHF outputs the current membrane potential value (i.e., Ouput MP) regardless of whether the spike is fired at each timestep. As a result, the IHF neuron outputs more information and makes the converter work well.
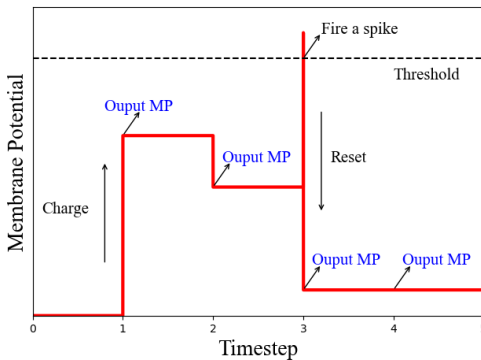

Fig. 2. The change of IHF membrane potential.

D. Training Strategy

Directly training the deep network with the JSCC model from scratch shows slow convergence [22]. We propose a three-step training strategy to fully train the entire model. For ease of understanding, we use S-JSCC to compress and transmit the feature of ResNet50 (Residual Network) [48] as an example to describe the training strategy. A similar training strategy can be used when S-JSCC is applied on other networks.

The first step is to train ResNet50 end-to-end using the cross-entropy loss function. After ResNet50 converges, we select an intermediate feature as the split point and split ResNet50 into the mobile device part and edge server part. The S-JSCC is placed at the split point to compress and transmit intermediate feature through digital channels.

The second step is to train the S-JSCC framework while keeping the parameters of the ResNet50 fixed. In this step, we use the surrogate gradient-based method to train the SNN, and the shifted Sigmoid function is utilized as the surrogate function of the firing step. In addition, we find that the firing rate of the feature in SNN affects the model performance [32]. Given (c, h, w) as the SNN feature dimension, the firing rate of the feature is modeled as

$$\text{Firing Rate} = \frac{\sum_{i=1}^{c} \sum_{j=1}^{h} \sum_{k=1}^{c} f(i, j, k)}{c * h * w}, \quad (4)$$

where the $f(i, j, k)$ is the spike value of the feature at the corresponding location. To constrain the firing rates of the compressed spiking features transmitted in the channel, we add a regularization term to the original loss function. So the loss function of the second step is modeled as

$$Loss = CrossEntropy + (\alpha - \text{Firing Rate})^2, \quad (5)$$

where α controls the expected firing rate of the compressed feature, and we set it as 0.5 according to the experiments.

The third step is to train the ResNet50 and S-JSCC jointly. These two trained models are combined together and finetuned end-to-end. The loss function of this step is the same as that of the second step, while the learning rate is lower.

IV. EXPERIMENTS AND RESULTS

A. Experiment Setup

In this paper, the whole model is trained and evaluated on CIFAR-100 [49] dataset for image classification. In CIFAR-100, 60,000 32×32 color images have 100 classes, with 600 images per class.

Moreover, we build ResNet50 using Pytorch [50], and S-JSCC is built by SpikingJelly [51], an open source deep learning framework for SNN based on PyTorch. The training and inferencing processes are carried out on Tesla V100 GPUs.

B. Baseline Method

The baseline method used in our experiments is a CNN-based JSCC framework, and the architecture of the baseline method is shown in Fig. 3.

The baseline method is an improved version of BottleNet++ [22], which can compress and transmit feature of the deep model over digital channel. In order to fit this model into the digital channel, the quantization step is placed at the end of the encoder. Since the output is constrained by the Sigmoid function in [0, 1], so the quantization is $X^q = round(X * (2^n - 1))$, where the floating-point X is represented

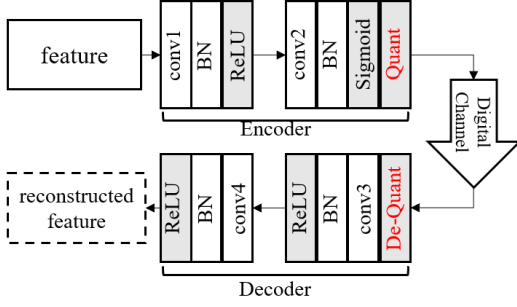Fig. 3. The architecture of the baseline method.

TABLE I
THE PARAMETER SETTING OF THE MODEL IN FIG. 1.

	Layer	Parameters
Encoder	conv1	kernel = 3, filter = 256
	conv2	kernel = 3, filter = 64
Decoder	conv3	kernel = 3, filter = 256
	conv4	kernel = 3, filter = 2048
Converter	FCNN	input = $2n$, output = 1

by an n-bit sequence. Correspondingly, the dequantization is $\bar{X} = X^q/(2^n - 1)$ at the decoder. In backpropagation, the quantization process is treated as an identity mapping.

C. Model Performance

In this section, both the S-JSCC model and the baseline model are used to compress and transmit the feature of the ResNet50 over digital channels. The split point we select is the output of the $14th$ bottleneck block, and the feature dimension is (2048, 4, 4). We keep the output dimension of the encoder the same in both approaches, i.e. (32, 4, 4). The parameter settings for encoder, decoder and converter in the S-JSCC model are shown in Table I. The baseline method uses the same settings in its encoder and decoder.

The trained ResNet50 in our experiment is the same as the ResNet50 used in BottleNet++, and the accuracy reaches 77.81%. In the second step, we train the S-JSCC model for 50 epochs with a batch size of 32, a learning rate of 10^{-4} and decayed by 2 every 10 epochs in the second step. In the third step, we train the whole model for 50 epochs with a batch size of 32, a learning rate of 10^{-5} and decayed by 2 every 10 epochs. The training details of the baseline method are the same except for the loss function in the second and third steps. The cross-entropy function is used to train baseline method all the time. In backpropagation, the noise interference of digital channels is treated as an identity mapping.

Moreover, to guarantee fairness, we compare the task performance and robustness of the ResNet50 with two different JSCC methods, under the condition that the number of bits transmitted through the channel is the same. For example, if baseline method uses n-bit quantization, then S-JSCC method will run n timesteps to transmit the same number of bits. In the following simulations, n is set as 4 and 8. We train the two models under BSC and BEC with different bit error/erasure rates and transmission overheads, then test their performance

under different channel conditions in Fig. 4. The evaluation metric is classification accuracy.

In the figures, $JSCC_{SNN}$ and $JSCC_{CNN}$ represent the test performance of the ResNet50 model combined with the proposed S-JSCC model and the baseline model, respectively. The solid and dashed lines in the same color indicate the performance of the ResNet50 with S-JSCC model and the baseline model trained under the same channel conditions.

In BSC, we trained two pairs of models with bit error rates (i.e., P_1) of 0.15 and 0.25, and we test the accuracy of these models over a range of bit error rates in Fig. 4(a) and Fig. 4(b). We find that the robustness of both $JSCC_{SNN}$ and $JSCC_{CNN}$ is improved when trained under a higher bit error rate, while the model accuracy at low bit error rates degrades. This phenomenon can be observed in both $n = 8$ and $n = 4$ scenarios. Moreover, although the model accuracy of $JSCC_{SNN}$ is slightly lower than $JSCC_{CNN}$ at low bit error rates (i.e., the accuracy decrease is lower than 1% when the bit error rate is lower than 0.1), $JSCC_{SNN}$ demonstrates very robust performance at high bit error rates (i.e., $JSCC_{SNN}$ outperforms $JSCC_{CNN}$ with an increase of 1.5%-2% on accuracy when bit error rate is higher than 0.2).

On the other hand, to prove the generality of the S-JSCC framework on different digital channels, we also train $JSCC_{SNN}$ and $JSCC_{CNN}$ on BEC with bit erasure rates (i.e., P_2) of 0.15 and 0.25 in Fig. 4(c) and Fig. 4(d). Because the channel nature of the BEC is different from that of the BSC, there is a 0.5 probability that the erased bits are not interfered with, as introduced in Section II-A. Therefore, the impact of the BEC on the bit sequence is smaller than that of the BSC. In the figure, the models are tested on a wider range of bit erasure rates, and the performance degrades significantly only when the bit erasure rate is greater than 0.3. Anyway, we can get a similar conclusion that $JSCC_{SNN}$ has close classification accuracy to $JSCC_{CNN}$ at low bit erasure rates, while $JSCC_{SNN}$ has much better performance than $JSCC_{CNN}$ at high bit erasure rates.

There are two reasons why S-JSCC outperforms the baseline method when the digital channel conditions are poor. One is that the weights of bits in the quantization result of the baseline method are different. The error of bit with a high weight may cause a large performance loss. However, S-JSCC does not have this problem. Another reason is that the SNN neurons only fire when the membrane potential exceeds the threshold, which also filters out some channel interference.

The experiment results prove that the S-JSCC framework is suitable for compressing and transmitting features over digital channels.

D. Ablation Studies

In this section, we aim to analyze the impact of the proposed IHF neuron and firing rate-based regularization method on model performance.

Base Model The basic form of the proposed S-JSCC framework is called the base model. In the base model, the decoder only outputs one decoded feature composed of spikes by the IF neuron, and all decoded features are input to the
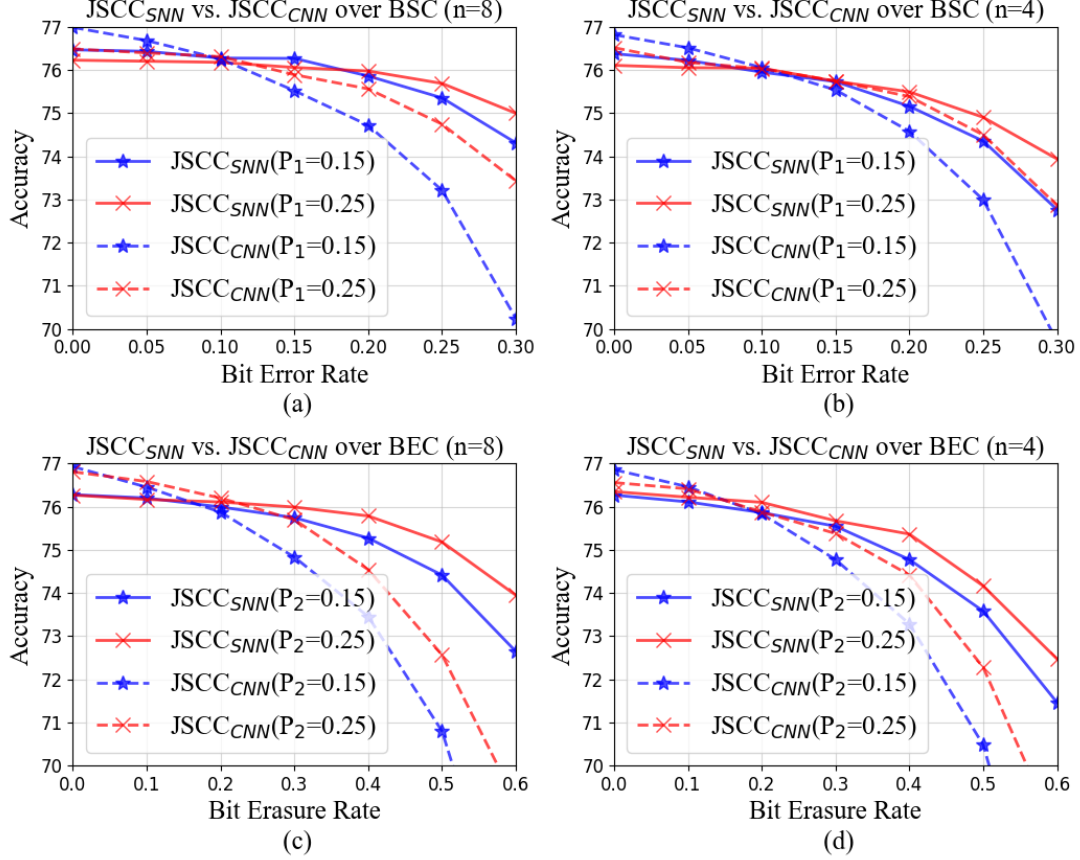
Fig. 4. Performance comparison between the S-JSCC and baseline over digital channels.

FCNN-based converter. In addition, the training strategy of the base model is similar to that before, except that the loss functions in the second and third steps do not add the regularization based on the firing rate.

IHF Model We replace the IF neuron at the end of the base model decoder with the IHF neuron, which is called the IHF model. The whole structure is the same as Fig. 1, but the training strategy is the same as base model.
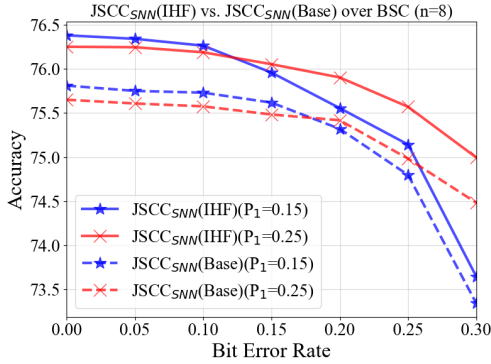

Fig. 5. Performance comparison between IHF model and base model over BSC.

We train the ResNet50 with base model and IHF model on the BSC with bit error rates of 0.15 and 0.25, and the test performance is shown in Fig. 5. In the figure, $JSCC_{SNN}$(IHF)

and $JSCC_{SNN}$(Base) represent the IHF model and base model, respectively. The solid and dashed lines in the same color indicate the performance of the ResNet50 with the S-JSCC model and the baseline model trained under the same channel conditions. We find that IHF model performs much better than base model over a wide range of bit error rates. The reason is that the output of the IHF contains more information than the output of the IF, enriching the input of the converter for weighted summation.

In conclusion, IHF neuron has a positive impact on improving model accuracy and robustness.

IHF+Reg Model Some SNN-related studies have shown that the firing rate of the spiking feature affects the performance of the model. However, the feature firing rate is not higher is better, and only an appropriate firing rate has a positive effect on the model performance.

Since IHF has been shown to have a positive effect on the model, we continued the ablation experiments based on the IHF model. This section mainly analyzes the effect of regularizing the firing rate of the compressed feature (i.e., the output of the encoder) during model training. We first count the firing rates of the compressed features of the trained IHF model, which uses the loss function without regularization and is trained on the BSC with a bit error rate of 0.15. Fig. 6 shows the statistical result.

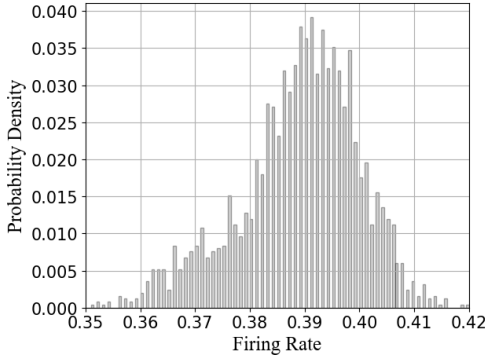From the figure, we find that the compressed feature firing

Fig. 6. The statistical result of compressed feature firing rates in IHF model.

rates are mainly concentrated around 0.388, which means only 38.8% of the spiking neurons are activated at each timestep. To explore the effect of different firing rates on model performance, we introduce the firing rate-based regularization term (i.e., $(\alpha - \text{Firing Rate})^2$) to constrain the compressed feature. We train IHF models with different α values in the regularization term, and we test them over a range of bit error rates. The IHF model with regularization is called the IHF+Reg model. The test results of the ResNet50 with different IHF+Reg models are shown in Fig. 7.
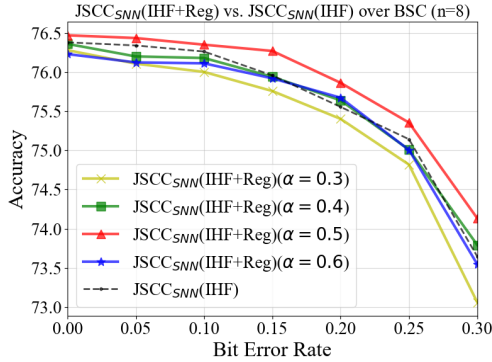

Fig. 7. Performance of the models with different regularization terms.

In Fig. 7, JSCC_{SNN}(IHF+Reg) represents the IHF+Reg model. The dotted line is the test performance of the IHF model, and the solid lines are the IHF+Reg models with different α values. We find that the performance and robustness of the model can be improved when the firing rate of the compressed feature is limited to 0.5.

The reason is that when the ratio of 0 and 1 in the compressed feature is the same, that is, the firing rate of the compressed feature is 0.5, the digital channel interference does not change the feature firing rate. Therefore, the model has the capability of resisting digital channel interference. On the contrary, when the proportions of 0 and 1 in the compressed feature are different, the digital channel interference changes the original proportion of 0 and 1 in the compressed feature, that is, changes the firing rate of the compressed feature, which affects the model performance.

In conclusion, regularizing the firing rates of the compressed

features to 0.5 also has a positive impact on model performance improvement.

V. CONCLUSION

Nowadays, the CNN-based JSCC technologies develop well, and they have shown excellent performance on analog channels. To design an JSCC framework for digital communication systems, we propose an SNN-based JSCC framework S-JSCC for compressing and transmitting deep features over digital channels. The S-JSCC framework can be directly applied on digital channels without an extra quantization step.

In this paper, we first build an SNN-based JSCC framework for transmitting features of deep models in CI scenarios. Then, we propose a novel spiking neuron called IHF and a firing rate-based regularization term for the loss function to improve the task performance and robustness of the model. Both IHF and the regularization term have been verified to have a positive impact on the model.

Finally, the S-JSCC framework is trained and tested on BSC and BEC, and the experiment results show that it performs better than the CNN-based JSCC framework on both BSC and BEC. Moreover, the proposed S-JSCC framework can be combined with most deep models in CI scenarios, and it is the first attempt to bridge the gap between SNN and digital communication.

REFERENCES

[1] Y. LeCun, Y. Bengio, and G. Hinton, "Deep learning," *nature*, vol. 521, no. 7553, pp. 436–444, 2015.

[2] Y. Kang, J. Hauswald, C. Gao, A. Rovinski, T. Mudge, J. Mars, and L. Tang, "Neurosurgeon: Collaborative intelligence between the cloud and mobile edge," *ACM SIGARCH Computer Architecture News*, vol. 45, no. 1, pp. 615–629, 2017.

[3] Z. Qin, H. Ye, G. Y. Li, and B.-H. F. Juang, "Deep learning in physical layer communications," *IEEE Wireless Communications*, vol. 26, no. 2, pp. 93–99, 2019.

[4] H. Choi and I. V. Bajić, "Deep feature compression for collaborative object detection," in *2018 25th IEEE International Conference on Image Processing (ICIP)*. IEEE, 2018, pp. 3743–3747.

[5] H. Choi and I. V. Bajić, "Near-lossless deep feature compression for collaborative intelligence," in *2018 IEEE 20th International Workshop on Multimedia Signal Processing (MMSP)*. IEEE, 2018, pp. 1–6.

[6] G. J. Sullivan, J.-R. Ohm, W.-J. Han, and T. Wiegand, "Overview of the high efficiency video coding (hevc) standard," *IEEE Transactions on circuits and systems for video technology*, vol. 22, no. 12, pp. 1649–1668, 2012.

[7] S. R. Alvar and I. V. Bajić, "Multi-task learning with compressible features for collaborative intelligence," in *2019 IEEE International Conference on Image Processing (ICIP)*. IEEE, 2019, pp. 1705–1709.

[8] S. R. Alvar and I. V. Bajić, "Bit allocation for multi-task collaborative intelligence," in *ICASSP 2020-2020 IEEE International Conference on Acoustics, Speech and Signal Processing (ICASSP)*. IEEE, 2020, pp. 4342–4346.

[9] G. Roelofs, *PNG: the definitive guide*. O'Reilly Media, 1999.

[10] A. Skodras, C. Christopoulos, and T. Ebrahimi, "The jpeg 2000 still image compression standard," *IEEE Signal processing magazine*, vol. 18, no. 5, pp. 36–58, 2001.

[11] Y. Wang, H. Yao, and S. Zhao, "Auto-encoder based dimensionality reduction," *Neurocomputing*, vol. 184, pp. 232–242, 2016.

[12] A. E. Eshratifar, A. Esmaili, and M. Pedram, "Towards collaborative intelligence friendly architectures for deep learning," in *20th International Symposium on Quality Electronic Design (ISQED)*. IEEE, 2019, pp. 14–19.

[13] A. E. Eshratifar, A. Esmaili, and M. Pedram, "Bottlenet: A deep learning architecture for intelligent mobile cloud computing services," in *2019 IEEE/ACM International Symposium on Low Power Electronics and Design (ISLPED)*. IEEE, 2019, pp. 1–6.

[14] Z. Zhang, M. Wang, M. Ma, J. Li, and X. Fan, "Msfc: Deep feature compression in multi-task network," in *2021 IEEE International Conference on Multimedia and Expo (ICME)*. IEEE, 2021, pp. 1–6.

[15] S. Kullback, *Information theory and statistics*. Courier Corporation, 1997.

[16] F. Zhai, Y. Eisenberg, and A. K. Katsaggelos, "Joint source-channel coding for video communications," *Handbook of Image and Video Processing*, pp. 1065–1082, 2005.

[17] E. Bourtsoulatze, D. B. Kurka, and D. Gündüz, "Deep joint source-channel coding for wireless image transmission," *IEEE Transactions on Cognitive Communications and Networking*, vol. 5, no. 3, pp. 567–579, 2019.

[18] M. Ding, J. Li, M. Ma, and X. Fan, "Snr-adaptive deep joint source-channel coding for wireless image transmission," in *ICASSP 2021-2021 IEEE International Conference on Acoustics, Speech and Signal Processing (ICASSP)*. IEEE, 2021, pp. 1555–1559.

[19] J. Xu, B. Ai, W. Chen, A. Yang, P. Sun, and M. Rodrigues, "Wireless image transmission using deep source channel coding with attention modules," *IEEE Transactions on Circuits and Systems for Video Technology*, vol. 32, no. 4, pp. 2315–2328, 2021.

[20] S. Wang, K. Yang, J. Dai, and K. Niu, "Distributed image transmission using deep joint source-channel coding," in *ICASSP 2022-2022 IEEE International Conference on Acoustics, Speech and Signal Processing (ICASSP)*. IEEE, 2022, pp. 5208–5212.

[21] M. Jankowski, D. Gündüz, and K. Mikolajczyk, "Deep joint source-channel coding for wireless image retrieval," in *ICASSP 2020-2020 IEEE International Conference on Acoustics, Speech and Signal Processing (ICASSP)*. IEEE, 2020, pp. 5070–5074.

[22] J. Shao and J. Zhang, "Bottlenet++: An end-to-end approach for feature compression in device-edge co-inference systems," in *2020 IEEE International Conference on Communications Workshops (ICC Workshops)*. IEEE, 2020, pp. 1–6.

[23] M. Wang, Z. Zhang, J. Li, M. Ma, and X. Fan, "Deep joint source-channel coding for multi-task network," *IEEE Signal Processing Letters*, vol. 28, pp. 1973–1977, 2021.

[24] P. Wang, J. Li, M. Ma, and X. Fan, "Distributed audio-visual parsing based on multimodal transformer and deep joint source channel coding," in *ICASSP 2022-2022 IEEE International Conference on Acoustics, Speech and Signal Processing (ICASSP)*. IEEE, 2022, pp. 4623–4627.

[25] W. Maass, "Networks of spiking neurons: the third generation of neural network models," *Neural networks*, vol. 10, no. 9, pp. 1659–1671, 1997.

[26] W. Fang, Z. Yu, Y. Chen, T. Masquelier, T. Huang, and Y. Tian, "Incorporating learnable membrane time constant to enhance learning of spiking neural networks," in *Proceedings of the IEEE/CVF International Conference on Computer Vision*, 2021, pp. 2661–2671.

[27] C. Xu, Y. Liu, and Y. Yang, "Direct training via backpropagation for ultra-low latency spiking neural networks with multi-threshold," *arXiv preprint arXiv:2112.07426*, 2021.

[28] J. Kim, H. Kim, S. Huh, J. Lee, and K. Choi, "Deep neural networks with weighted spikes," *Neurocomputing*, vol. 311, pp. 373–386, 2018.

[29] Y. Chen, Y. Mai, R. Feng, and J. Xiao, "An adaptive threshold mechanism for accurate and efficient deep spiking convolutional neural networks," *Neurocomputing*, vol. 469, pp. 189–197, 2022.

[30] K. Patel, E. Hunsberger, S. Batir, and C. Eliasmith, "A spiking neural network for image segmentation," *arXiv preprint arXiv:2106.08921*, 2021.

[31] S. Kim, S. Park, B. Na, and S. Yoon, "Spiking-yolo: spiking neural network for energy-efficient object detection," in *Proceedings of the AAAI conference on artificial intelligence*, vol. 34, no. 07, 2020, pp. 11270–11277.

[32] Y. Cao, Y. Chen, and D. Khosla, "Spiking deep convolutional neural networks for energy-efficient object recognition," *International Journal of Computer Vision*, vol. 113, no. 1, pp. 54–66, 2015.

[33] W. Fang, Z. Yu, Y. Chen, T. Huang, T. Masquelier, and Y. Tian, "Deep residual learning in spiking neural networks," *Advances in Neural Information Processing Systems*, vol. 34, pp. 21056–21069, 2021.

[34] N. Skatchkovsky, H. Jang, and O. Simeone, "End-to-end learning of neuromorphic wireless systems for low-power edge artificial intelligence," in *2020 54th Asilomar Conference on Signals, Systems, and Computers*. IEEE, 2020, pp. 166–173.

[35] K. Choi, K. Tatwawadi, A. Grover, T. Weissman, and S. Ermon, "Neural joint source-channel coding," in *International Conference on Machine Learning*. PMLR, 2019, pp. 1182–1192.

[36] S. Lu and A. Sengupta, "Exploring the connection between binary and spiking neural networks," *Frontiers in Neuroscience*, vol. 14, p. 535, 2020.

[37] W. Gerstner, W. M. Kistler, R. Naud, and L. Paninski, *Neuronal dynamics: From single neurons to networks and models of cognition*. Cambridge University Press, 2014.

[38] E. Ledinauskas, J. Ruseckas, A. Juršėnas, and G. Buračas, "Training deep spiking neural networks," *arXiv preprint arXiv:2006.04436*, 2020.

[39] B. Han, G. Srinivasan, and K. Roy, "Rmp-snn: Residual membrane potential neuron for enabling deeper high-accuracy and low-latency spiking neural network," in *Proceedings of the IEEE/CVF conference on computer vision and pattern recognition*, 2020, pp. 13558–13567.

[40] L. Zhu, X. Wang, Y. Chang, J. Li, T. Huang, and Y. Tian, "Event-based video reconstruction via potential-assisted spiking neural network," in *Proceedings of the IEEE/CVF Conference on Computer Vision and Pattern Recognition*, 2022, pp. 3594–3604.

[41] Z. Wu, H. Zhang, Y. Lin, G. Li, M. Wang, and Y. Tang, "Liaf-net: Leaky integrate and analog fire network for lightweight and efficient spatiotemporal information processing," *IEEE Transactions on Neural Networks and Learning Systems*, 2021.

[42] H. Jang, N. Skatchkovsky, and O. Simeone, "Spiking neural networks—part i: Detecting spatial patterns," *IEEE Communications Letters*, vol. 25, no. 6, pp. 1736–1740, 2021.

[43] B. Rueckauer, I.-A. Lungu, Y. Hu, M. Pfeiffer, and S.-C. Liu, "Conversion of continuous-valued deep networks to efficient event-driven networks for image classification," *Frontiers in neuroscience*, vol. 11, p. 682, 2017.

[44] W. Fang, Z. Yu, Y. Chen, T. Huang, T. Masquelier, and Y. Tian, "Deep residual learning in spiking neural networks," *Advances in Neural Information Processing Systems*, vol. 34, pp. 21056–21069, 2021.

[45] Y. Wu, L. Deng, G. Li, J. Zhu, Y. Xie, and L. Shi, "Direct training for spiking neural networks: Faster, larger, better," in *Proceedings of the AAAI Conference on Artificial Intelligence*, vol. 33, no. 01, 2019, pp. 1311–1318.

[46] S.-i. Ikegawa, R. Saiin, Y. Sawada, and N. Natori, "Rethinking the role of normalization and residual blocks for spiking neural networks," *Sensors*, vol. 22, no. 8, p. 2876, 2022.

[47] N. Rathi and K. Roy, "Diet-snn: A low-latency spiking neural network with direct input encoding and leakage and threshold optimization," *IEEE Transactions on Neural Networks and Learning Systems*, 2021.

[48] K. He, X. Zhang, S. Ren, and J. Sun, "Deep residual learning for image recognition," in *Proceedings of the IEEE conference on computer vision and pattern recognition*, 2016, pp. 770–778.

[49] A. Krizhevsky, G. Hinton *et al.*, "Learning multiple layers of features from tiny images," 2009.

[50] A. Paszke, S. Gross, F. Massa, A. Lerer, J. Bradbury, G. Chanan, T. Killeen, Z. Lin, N. Gimelshein, L. Antiga *et al.*, "Pytorch: An imperative style, high-performance deep learning library," *Advances in neural information processing systems*, vol. 32, 2019.

[51] W. Fang, Y. Chen, J. Ding, D. Chen, Z. Yu, H. Zhou, Y. Tian, and other contributors, "Spikingjelly," https://github.com/fangwei123456/spikingjelly, 2020, accessed: 2021-07-03.